

1
2 **Selective Alteration of the Root Morphology of**
3 ***Arabidopsis thaliana* by Synthetic Anion**
4 **Transporters (SATs)**

5
6 **Mohit B. Patel,^{1,2} Evan C. Garrad,² Steven Korb,² Saeedeh Negin,¹**
7 **Michael R. Gokel,¹ Sergey Sedinkin,¹ Shanheng “Andrew” Yin,¹ and**
8 **George W. Gokel^{1,2*}**

9
10 ¹*Department of Chemistry & Biochemistry, University of Missouri – St. Louis, 1 University*
11 *Blvd., St. Louis, MO 63121 U. S. A.*

12 ²*Department of Biology, University of Missouri – St. Louis, 1 University Blvd., St. Louis, MO*
13 *63121 U. S. A.*

14
15
16
17 **ABSTRACT**

Aims: The aim of the study was to determine whether and to what extent any of a family of amphiphilic heptapeptide synthetic anion transporters (SATs) affected the growth or root morphology of *Arabidopsis thaliana*.

Study design: *A. thaliana* plants were grown from seedlings in PNS media in the absence or presence of one of 21 SATs.

Place and Duration of Study: Departments of Chemistry & Biochemistry, University of Missouri – St. Louis, 1 University Blvd., St. Louis, MO 63121 U. S. A. The study was conducted 2017-2018.

Methodology: Twenty one compounds of the form R₂N-COCH₂YCH₂CO-(Aaa)₃Pro(Aaa)₃-O(CH₂)₆CH₃ were prepared and studied. The amino acids included Ala, Gly, and Ser. R was normal alkyl having 6, 10, 12, or 18 carbons. Y was methylene, oxygen, sulfur, or absent. The PNS media was infused with various concentrations of the SAT and 21 plants in each group were allowed to grow for 11 days. Overall plant growth and root morphology were visualized and/or measured and the results recorded.

Results: A comparison of primary root length and lateral root number revealed that the greatest alterations in lateral root densities were observed for peptide sequences of the type GGGPSGS, whether or not serine was protected by *t*-butyl. Differences were also observed for these peptide sequences according to the identity of Y in the ~COCH₂YCH₂CO~ chain.

Conclusion: The presence of serine's oxygen atoms on the C-terminal side of the heptapeptide interact with Cl⁻ leading to a change in ion concentrations and alterations in primary root lengths and lateral root densities.

18
19 *Keywords: amphiphile, Arabidopsis thaliana, heptapeptide, lateral root density, synthetic anion transporter, synthetic ion*
20 *channel*

21
22
23
24 **1. INTRODUCTION**

25
26 During recent decades, extensive study has been reported of biological effects of ion binders and transporters, particularly
27 of cation complexers on bacteria and fungi.[1] Within the crown ether class of ion binders and transporters, biological

effects have been reported involving microbes,[2] tissues,[3] plants,[4] and animals.[5] Although several reports relate to studies of whole plants, this remains a poorly explored area.

We recently reported the effect of hydrophile and lariat ether synthetic cation transporters on the growth of *Arabidopsis thaliana*.^[6,7] These cation binders and transporters showed significant effects on *A. thaliana* root morphology. The effect mimicked the action of the growth hormone indoleacetic acid, albeit at a much higher concentration than observed with the natural hormone. More detailed study revealed that the transporters were not true growth hormone mimics. Our surmise was that the observed behavior related to changes in ion balance mediated to greater or lesser extents by the efficacy of the transporter.

Although only limited studies have been reported of interactions between alkali metal ion carriers and/or transporters, factors affecting root morphology has been an area of interest for some time. This includes studies of root alterations caused by chemical excesses or deficiencies in maize,^[8] in *Medicago sativa* L.,^[9] and the Brazilian medicinal plant *Pfaffia glomerata*.^[10] In the latter case, the presence of zinc metal was the focus of study. Notwithstanding, research on the interactions of alkali metal ion binders such as cryptands and crown ethers with vital plants are almost unknown. Other recent studies include examinations of copper toxicity to grapevine^[11] and cation effects on banana root segments.^[12] The effect of the polyamine cadaverine on *A. thaliana* has recently been reported.^[13]

The class of compounds we have called synthetic anion transporters (SATs)^[14] were designed and confirmed to transport Cl⁻ through phospholipid bilayer membranes.^[15] The SATs were designed based on the putative chloride selectivity sequence of the ClC family of proteins. This led to the selection of G₃PG₃ peptide sequence.^[16] Since the peptide must insert in membranes, an anchoring module was added to the N-terminal end of the peptide. The initial module was [CH₃(CH₂)₁₇]₂N. Reaction of the secondary amine with diglycolic anhydride produced the entire anchor module, (C₁₈H₃₇)₂NCOCH₂OCH₂COOH in a single step. This module corresponds in dimension and polarity to the corresponding segment of distearoylphosphatidylcholine. Heptanol was determined by experiment to be the most effective C-terminal secondary anchor that would also block the unlinked glycine carboxyl.^[17]

The SATs show Cl⁻-selective release from liposomes and open-close behavior characteristic of protein chloride channels.^[18] When the anchor chains were C₁₈, Cl⁻ ion selectivity was high, but it diminished as the primary anchor chains were shortened.^[19] The original diglycolic acid module was replaced by glutaric acid, succinic acid, and thiodiglycolic acid.^[20] Surprisingly, SATs containing succinic acid proved to be the most active ion transporters. Biophysical studies confirmed membrane insertion and the formation of a dimeric pore.^[21]

To our knowledge, previous studies of effects on plants by ion binding agents^[4a,c] focused on the complexation and/or transport of cations, specifically sodium and potassium, that could affect plant growth dynamics. The investigation reported here was initiated to discover if and to what extent altering anion balance, in particular Cl⁻, would affect root morphology or any other plant phenotype. The results of those studies follow.

2. MATERIAL AND METHODS / EXPERIMENTAL DETAILS / METHODOLOGY

2.1 General.

¹H-NMR were recorded at 300 MHz in CDCl₃ solvents and are reported in ppm (*delta*) downfield from internal (CH₃)₃Si. ¹³C-NMR were recorded at corresponding frequencies in CDCl₃ unless otherwise stated. Melting points were determined on a Thomas Hoover apparatus in open capillaries and are uncorrected. Thin layer chromatographic (TLC) analyses were performed on aluminum oxide 60 F-254 neutral (Type E) with a 0.2 mm layer thickness or on silica gel 60 F-254 with a 0.2 mm layer thickness. Preparative chromatography columns were packed with activated aluminum oxide (MCB 80-325 mesh, chromatographic grade, AX 611) or with Kieselgel 60 (70-230 mesh). All reactions were conducted under dry N₂ unless otherwise stated. All reagents were the best (non-LC) grade commercially available and were distilled, recrystallized, or used without further purification, as appropriate.

2.2 Preparation of (C₆H₁₃)₂NCOCH₂CH₂CO(Gly)₃Pro(Gly)₃OC₇H₁₅, **1**.

(C₆H₁₃)₂NCOCH₂CH₂CO(Gly)₃OH (160 mg, 0.350 mmol) was dissolved in DMF (5 mL) in a 25 mL rb flask. The mixture was cooled to 0 °C and 2,4,6-trimethylpyridine (140 μL) and HBTU (140 mg) were added. The mixture was stirred for 30 min and H-Pro(Gly)₃OC₇H₁₅ (150 mg) was added. The mixture was stirred at rt for 16 h. The mixture was diluted with CH₂Cl₂ (250 mL) and washed with 250 mL each of the following: H₂O, 1M NaHSO₄, H₂O × 3, 5% NaHCO₃, and H₂O. The CH₂Cl₂ solution was filtered through a 1:1 celite/MgSO₄ mixture. The solution was evaporated and chromatographed over a column of SiO₂ (eluent: 0%-20% MeOH in CHCl₃). Evaporation of the solvent followed by high vacuum for 16 h afforded **1** as a white solid (243 mg, 84% yield). MP: 85-90 °C. ¹H NMR: 0.8 (t, 9H); 1.19 (m, 20H); 1.37 (bs, 3H); 1.61 (bs, 3H); 2.37 (t, 2H); 2.74 (t, 2H); 3.14 (t, 4H); 3.89 (m, 8H); 4.08 (m, 2H); 6.48 (s, 1H); 7.02 (s, 1H); 8.12 (s, 1H) ppm.

2.3 Preparation of (C₁₀H₂₁)₂NCOCH₂CH₂CO(Gly)₃Pro(Gly)₃-OC₇H₁₅, 2.

(C₁₀H₂₁)₂NCOCH₂CH₂CO(Gly)₃OH (300 mg, 0.527 mmol) was dissolved in DMF (5 mL) in a 25 mL rb flask. The mixture was cooled to 0 °C and 2,4,6-trimethylpyridine (210 μL) and HBTU (210 mg) were added. The mixture was stirred for 30 min and H-Pro(Gly)₃-OC₇H₁₅ (222 mg) was added. The mixture was stirred at rt for 16 h. The mixture was diluted with CH₂Cl₂ (250 mL) and washed with 250 mL each of the following: H₂O, 1M NaHSO₄, H₂O × 3, 5% NaHCO₃, and H₂O. The CH₂Cl₂ solution was filtered through a 1:1 celite/MgSO₄ mixture. The solution was evaporated and chromatographed over a column of SiO₂ (eluent: 0%-20% MeOH in CHCl₃). Evaporation of the solvent followed by high vacuum for 16 h afforded **2** as a white solid (433 mg, 88% yield). MP: 147-152 °C. ¹H NMR: 0.81 (t, 9H); 1.17 (bs, 36H); 1.36 (bs, 2H); 1.55 (bs, 4H); 1.93-2.14 (m, 4H); 2.33 (m, 1H); 2.57 (m, 2H); 2.75 (m, 1H); 3.13 (bs, 4H); 3.62 (m, 6H); 3.85 (d, 1H); 4.16 (m, 8H); 7.35 (bs, 2H); 7.46 (bs, 1H); 7.89 (bs, 1H); 8.17 (bs, 1H) ppm.

2.4 Preparation of (C₁₂H₂₃)₂NCOCH₂CH₂CO(Gly)₃Pro(Gly)₃-OC₇H₁₅, 3.

(C₁₂H₂₃)₂NCOCH₂CH₂CO(Gly)₃OH (300 mg, 0.480 mmol) was dissolved in DMF (5 mL) in a 25 mL rb flask. The mixture was cooled to 0 °C and 2,4,6-trimethylpyridine (190 μL) and HBTU (191 mg) were added. The mixture was stirred for 30 min and H-Pro(Gly)₃-OC₇H₁₅ (202 mg) was added. The mixture was stirred at rt for 16 h. The mixture was diluted with CH₂Cl₂ (250 mL) and washed with 250 mL each of the following: H₂O, 1M NaHSO₄, H₂O × 3, 5% NaHCO₃, and H₂O. The CH₂Cl₂ solution was filtered through a 1:1 celite/MgSO₄ mixture. The solution was evaporated and chromatographed over a column of SiO₂ (eluent: 0%-20% MeOH in CHCl₃). Evaporation of the solvent followed by high vacuum for 16 h afforded **3** as a white solid (412 mg, 86% yield). MP: 147-151 °C. ¹H NMR: 0.92 (t, 9H); 1.29 (bs, 44H); 1.47 (bs, 2H); 1.65 (bs, 4H); 2.04 (s, 2H); 2.25 (m, 2H); 2.39 (m, 2H); 2.44 (m, 1H); 2.60-2.80 (m, 2H); 2.90 (m, 1H); 3.24 (bs, 4H); 3.62 (m, 6H); 3.97 (d, 1H); 4.14 (m, 8H); 7.44 (bs, 3H); 8.03 (bs, 1H); 8.29 (bs, 1H) ppm.

2.5 Preparation of (C₁₈H₃₇)₂NCOCH₂CH₂CO(Gly)₃Pro(Gly)₃-OC₇H₁₅, 4.

(C₁₈H₃₇)₂NCOCH₂CH₂CO(Gly)₃OH (309 mg, 0.390 mmol) and 184 mg H-Pro(Gly)₃-OC₇H₁₅ were dissolved in CH₂Cl₂ (5 mL containing 64 mg *n*-butanol) in a 25 mL rb flask. The mixture was cooled to 0 °C and EDCI (81 mg) and triethylamine (0.21 mL) were added. The mixture was stirred at rt under argon for 16 h. The mixture was diluted with CH₂Cl₂ (100 mL) and washed with 100 mL each of the following: H₂O, 1M NaHSO₄, H₂O, 5% NaHCO₃, and H₂O. The CH₂Cl₂ solution was filtered through a 1:1 celite/MgSO₄ mixture. The solution was evaporated and chromatographed over a column of SiO₂ (eluent: 5%-15% MeOH in CHCl₃). Evaporation followed by high vacuum for 16 h afforded **4** as a white solid (356 mg, 79% yield). MP: 148-152 °C. ¹H NMR: 0.87 (m, 12H), 1.25 (m, 72H), 1.42 (br s, 2H), 1.55 (br s, 2H), 1.80-2.40 (m, 4H), 2.40-2.80 (m, 4H), 3.22 (br s, 4H), 3.25-4.40 (m, 15H), 7.45 (br s, 2H), 7.73 (br s, 1H), 8.14 (s, 2H).

2.6 Preparation of (C₆H₁₃)₂NCOCH₂OCH₂CO(Gly)₃Pro(Gly)₃-OC₇H₁₅, 5, was prepared as previously reported.[15]

2.7 Preparation of (C₁₈H₃₇)₂NCOCH₂OCH₂CO(Gly)₃Pro(Gly)₃-OC₇H₁₅, 6, was prepared as previously reported.[28]

2.8 Preparation of (C₁₂H₂₃)₂NCOCH₂CH₂CO(Ala)₃Pro(Gly)₃-OC₇H₁₅, 7.

(C₁₂H₂₃)₂NCOCH₂CH₂CO(Ala)₃OH (62 mg, 0.093 mmol) and 82 mg H-Pro(Gly)₃-OC₇H₁₅ were dissolved in DMF (5 mL) in a 25 mL rb flask. The mixture was cooled to 0 °C and 2,4,6-trimethylpyridine (55 μL) and HBTU (55 mg) were added. The mixture was stirred at rt for 16 h. The mixture was diluted with CH₂Cl₂ (150 mL) and washed with 150 mL each of the following: H₂O, 1M NaHSO₄, H₂O × 3, 5% NaHCO₃, and H₂O. The CH₂Cl₂ solution was filtered through a 1:1 celite/MgSO₄ mixture. The solution was evaporated and chromatographed over a column of SiO₂ (eluent: 0%-10% MeOH in CHCl₃). Evaporation of the solvent followed by high vacuum for 16 h afforded **7** as a white solid (101 mg, 71% yield). MP: 130-135 °C. ¹H NMR: 0.81 (t, 13H); 1.19 (bs, 73H); 1.40 (bs, 15H); 1.84-2.16 (m, 6H); 2.34 (s, 2H); 2.61 (m, 3H); 2.80-3.16 (m, 7H); 3.57 (m, 3H); 3.90 (m, 9H); 4.28 (m, 5H); 6.15 (d, 1H); 7.50 (t, 1H); 7.68 (d, 1H); 7.86 (t, 1H) ppm.

2.9 Preparation of (C₁₈H₃₇)₂NCOCH₂CH₂CO(Ala)₃Pro(Gly)₃-OC₇H₁₅, 8.

(C₁₈H₃₇)₂NCOCH₂CH₂CO(Ala)₃OH (62 mg, 0.102 mmol) and 82 mg H-Pro(Gly)₃-OC₇H₁₅ were dissolved in DMF (5 mL) in a 25 mL rb flask. The mixture was cooled to 0 °C and 2,4,6-trimethylpyridine (55 μL) and HBTU (55 mg) were added. The mixture was stirred at rt for 16 h. The mixture was diluted with CH₂Cl₂ (150 mL) and washed with 150 mL each of the following: H₂O, 1M NaHSO₄, H₂O × 3, 5% NaHCO₃, and H₂O. The CH₂Cl₂ solution was filtered through a 1:1 celite/MgSO₄ mixture. The solution was evaporated and chromatographed over a column of SiO₂ (eluent: 0%-10% MeOH in CHCl₃). Evaporation of the solvent followed by high vacuum for 16 h afforded **8** as a white solid (120 mg, 73% yield). MP: 153-157 °C. ¹H NMR: 0.92 (t, 12H); 1.31 (bs, 96H); 1.49 (bs, 14H); 1.94-2.26 (m, 7H); 2.45 (s, 2H); 2.71 (m, 2H); 3.25-3.33 (m, 7H); 3.71 (m, 3H); 4.39-4.54 (m, 14H); 6.37 (d, 1H); 7.31 (t, 2H); 7.75 (d, 2H); 8.00 (t, 1H) ppm.

146 **2.10 Preparation of (C₁₂H₂₃)₂NCOCH₂OCH₂CO(Ala)₃Pro(Gly)₃-OC₇H₁₅, **9**.**

147 (C₁₂H₂₃)₂NCOCH₂OCH₂CO(Ala)₃OH (186 mg, 0.272 mmol) and 237 mg H-Pro(Gly)₃-OC₇H₁₅ were dissolved in DMF (5
148 mL) in a 25 mL rb flask. The mixture was cooled to 0 °C and 2,4,6-trimethylpyridine (160 μL) and HBTU (160 mg) were
149 added. The mixture was stirred at rt for 16 h. The mixture was diluted with CH₂Cl₂ (150 mL) and washed with 150 mL
150 each of the following: H₂O, 1M NaHSO₄, H₂O × 3, 5% NaHCO₃, and H₂O. The CH₂Cl₂ solution was filtered through a 1:1
151 celite/MgSO₄ mixture. The solution was evaporated and chromatographed over a column of SiO₂ (eluent: 0%-10% MeOH
152 in CHCl₃). Evaporation of the solvent followed by high vacuum for 16 h afforded **9** as a white solid (101 mg, 71% yield).
153 MP: 128-134 °C. ¹H NMR: 0.92 (t, 9H); 1.29 (bs, 54H); 1.50 (m, 10H); 2.16 (m, 6H); 3.11-3.82 (m, 6H); 4.11 (m, 8H); 4.51
154 (m, 7H); 7.31 (m, 2H); 7.66 (d, 2H); 7.85 (d, 1H); 7.99 (t, 1H) ppm.

155
156 **2.11 Preparation of (C₁₈H₃₇)₂NCOCH₂OCH₂CO(Ala)₃Pro(Gly)₃-OC₇H₁₅, **10**.**

157 (C₁₈H₃₇)₂NCOCH₂OCH₂CO(Ala)₃OH (253 mg, 0.297 mmol) and 237 mg H-Pro(Gly)₃-OC₇H₁₅ were dissolved in DMF (5
158 mL) in a 25 mL rb flask. The mixture was cooled to 0 °C and 2,4,6-trimethylpyridine (160 μL) and HBTU (160 mg) were
159 added. The mixture was stirred at rt for 16 h. The mixture was diluted with CH₂Cl₂ (150 mL) and washed with 150 mL
160 each of the following: H₂O, 1M NaHSO₄, H₂O × 3, 5% NaHCO₃, and H₂O. The CH₂Cl₂ solution was filtered through a 1:1
161 celite/MgSO₄ mixture. The solution was evaporated and chromatographed over a column of SiO₂ (eluent: 0%-10% MeOH
162 in CHCl₃). Evaporation of the solvent followed by high vacuum for 16 h afforded **10** as a white solid (409 mg, 85% yield).
163 MP: 126-130 °C. ¹H NMR: 0.80 (t, 10H); 1.18 (bs, 85H); 1.38 (bs, 10H); 1.87 (m, 2H); 2.06 (bs, 7H); 2.99 (m, 4H); 3.53
164 (m, 2H); 3.81 (m, 10H); 4.23 (m, 8H); 7.20 (m, 2H); 7.57 (d, 1H); 7.67 (t, 1H); 7.75 (d, 1H); 7.90 (t, 1H) ppm.

165
166 **2.12 Preparation of (C₁₈H₃₇)₂NCOCH₂SCH₂CO(Ala)₃Pro(Gly)₃-OC₇H₁₅, **11**.**

167 (C₁₈H₃₇)₂NCOCH₂SCH₂CO(Ala)₃OH (127 mg, 0.297 mmol) and 116 mg H-Pro(Gly)₃-OC₇H₁₅ were dissolved in DMF (5
168 mL) in a 25 mL rb flask. The mixture was cooled to 0 °C and 2,4,6-trimethylpyridine (50 μL) and HBTU (77 mg) were
169 added. The mixture was stirred at rt for 16 h. The mixture was diluted with CH₂Cl₂ (150 mL) and washed with 150 mL
170 each of the following: H₂O, 1M NaHSO₄, H₂O × 3, 5% NaHCO₃, and H₂O. The CH₂Cl₂ solution was filtered through a 1:1
171 celite/MgSO₄ mixture. The solution was evaporated and chromatographed over a column of SiO₂ (eluent: 0%-10% MeOH
172 in CHCl₃). Evaporation of the solvent followed by high vacuum for 16 h afforded **11** as a white solid (183 mg, 76% yield).
173 MP: 154-158 °C. ¹H NMR: 0.88 (t, 9H); 1.28 (bs, 68H); 1.39 (bs, 2H); 1.65 (bs, 4H); 1.97-2.17 (s, 4H); 2.95-4.10 (m, 18H);
174 4.38 (m, 3H); 4.66 (m, 1H); 7.48 (bs, 2H); 7.65 (bs, 1H); 8.01 (bs, 1H); 8.14 (bs, 2H) ppm.

175
176 **2.13 Preparation of (C₁₂H₂₃)₂NCOCH₂CH₂CO(Gly)₃ProSerGlySer-OC₇H₁₅, **12**.**

177 (C₁₂H₂₃)₂NCOCH₂CH₂CO(Gly)₃ProGlySer(*t*-Bu)Gly-OC₇H₁₅ (205 mg, 0.195 mmol) was dissolved in dioxane (2 mL). The
178 mixture was cooled and stirred to 0 °C and 4M HCl in dioxane (1 mL) was added. The mixture was stirred at 0 °C for 2 h.
179 The solvent was evaporated followed by high vacuum for 16 h afforded **12** as a white solid (160 mg, 80% yield). MP: 129-
180 134 °C. ¹H NMR: 0.80 (t, 10H); 1.07 (s, 4H); 1.21 (bs, 68H); 1.36 (bs, 6H); 1.91-2.43 (m, 10H); 3.13 (bs, 4H); 3.48-4.10
181 (m, 17H); 4.53 (m, 1H); 7.40-8.40 (m, 6H) ppm.

182
183 **2.14 Preparation of (C₁₈H₃₇)₂NCOCH₂CH₂CO(Gly)₃ProSerGlySer-OC₇H₁₅, **13**.**

184 (C₁₈H₃₇)₂NCOCH₂CH₂CO(Gly)₃ProSer(*t*-Bu)GlySer(*t*-Bu)-OC₇H₁₅ (200 mg, 0.164 mmol) was dissolved in Dioxane (2 mL).
185 The mixture was cooled and stirred to 0 °C and 4M HCl in dioxane (1 mL) was added. The mixture was stirred at 0 °C for
186 2 h. The solvent was evaporated followed by high vacuum for 16 h afforded **13** as a white solid (146 mg, 75%). MP: 145-
187 150 °C. ¹H NMR: 0.80 (t, 10H); 1.07 (s, 4H); 1.21 (bs, 68H); 1.36 (bs, 6H); 1.91-2.43 (m, 10H); 3.13 (bs, 4H); 3.48-4.10
188 (m, 17H); 4.53 (m, 1H); 7.40-8.40 (m, 6H) ppm.

189
190 **2.15 Preparation of (C₁₈H₃₇)₂NCOCH₂OCH₂CO(Gly)₃ProSerGlySer-OC₇H₁₅, **14**.**

191 (C₁₈H₃₇)₂NCOCH₂OCH₂CO(Gly)₃ProSer(*t*-Bu)GlySer(*t*-Bu)-OC₇H₁₅ (200 mg, 0.162 mmol) was dissolved in dioxane (2
192 mL). The mixture was cooled and stirred to 0 °C and 4M HCl in dioxane (1 mL) was added. The mixture was stirred at 0
193 °C for 2 h. The solvent was evaporated, followed by high vacuum for 16 h afforded **14** as a white solid (165 mg, 85%).
194 MP: 74-78 °C. ¹H NMR: 0.80 (t, 10H); 1.08 (s, 4H); 1.18 (bs, 68H); 1.44 (d, 6H); 1.96 (bs, 10H); 3.00 (m, 2H); 3.20 (bs,
195 2H); 3.46 (bs, 1H); 3.91 (m, 10H); 4.22 (m, 4H); 7.40-8.49 (m, 6H) ppm.

196
197 **2.16 Preparation of (C₁₂H₂₃)₂NCOCH₂CH₂CO(Gly)₃ProSer(*t*-Bu)GlySer(*t*-Bu)-OC₇H₁₅, **15**.**

198 (C₁₂H₂₃)₂NCOCH₂CH₂CO(Gly)₃OH (224 mg, 0.358 mmol) and 200 mg H-ProSer(*t*-Bu)GlySer(*t*-Bu)-OC₇H₁₅ were dissolved
199 in DMF (10 mL) in a 25 mL rb flask. The mixture was cooled to 0 °C and 2,4,6-trimethylpyridine (140 μL) and HBTU (143
200 mg) were added. The mixture was stirred at rt for 16 h. The mixture was diluted with CH₂Cl₂ (150 mL) and washed with
201 150 mL each of the following: H₂O, 1M NaHSO₄, H₂O × 3, 5% NaHCO₃, and H₂O. The CH₂Cl₂ solution was filtered
202 through a 1:1 celite/MgSO₄ mixture. The solution was evaporated and chromatographed over a column of SiO₂ (eluent:
203 0%-10% MeOH in CHCl₃). Evaporation of the solvent followed by high vacuum for 16 h afforded **15** as a white solid (375

204 mg, 90% yield). MP: 109-111 °C. ¹H NMR: 0.88 (t, 9H); 1.16 (d, 24H); 1.26 (bs, 44H); 1.45 (bs, 2H); 1.60 (bs, 4H); 2.08 (s, 4H); 2.57 (m, 4H); 3.23 (bs, 4H); 3.57-4.19 (m, 17H); 7.49 (bs, 1H); 7.61 (bs, 1H); 7.75 (bs, 1H); 7.87 (bs, 2H); 8.17 (bs, 1H) ppm.

2.17 Preparation of (C₁₈H₃₇)₂NCOCH₂CH₂CO(Gly)₃ProSer(*t*-Bu)GlySer(*t*-Bu)-OC₇H₁₅, **16**.

209 (C₁₈H₃₇)₂NCOCH₂CH₂CO(Gly)₃OH (278 mg, 0.350 mmol) and 193 mg H-ProSer(*t*-Bu)GlySer(*t*-Bu)-OC₇H₁₅ were dissolved in DMF (10 mL) in a 25 mL rb flask. The mixture was cooled to 0 °C and 2,4,6-trimethylpyridine (140 μL) and HBTU (138 mg) were added. The mixture was stirred at rt for 16 h. The mixture was diluted with CH₂Cl₂ (150 mL) and washed with 150 mL each of the following: H₂O, 1M NaHSO₄, H₂O × 3, 5% NaHCO₃, and H₂O. The dichloromethane solution was filtered through a 1:1 celite/MgSO₄ mixture. The solution was evaporated and chromatographed over a column of SiO₂ (eluent: 0%-10% MeOH in CHCl₃). Evaporation of the solvent followed by high vacuum for 16 h afforded **16** as a white solid (406 mg, 88% yield). MP: 108-110 °C. ¹H NMR: 0.80 (t, 11H); 1.07 (d, 20H); 1.18 (bs, 82H); 1.35 (bs, 3H); 1.50 (m, 5H); 1.94 (m, 7H); 2.37-2.80 (m, 4H); 3.12 (m, 5H); 3.44-4.26 (m, 20H); 4.49 (m, 1H); 6.92 (d, 1H); 7.12 (d, 1H); 7.25 (t, 1H); 7.72 (t, 1H); 7.78 (t, 1H); 8.14 (t, 1H) ppm.

2.18 Preparation of (C₁₂H₂₃)₂NCOCH₂OCH₂CO(Gly)₃ProSer(*t*-Bu)GlySer(*t*-Bu)-OC₇H₁₅, **17**.

220 (C₁₂H₂₃)₂NCOCH₂OCH₂CO(Gly)₃OH (230 mg, 0.359 mmol) and 200 mg H-ProSer(*t*-Bu)GlySer(*t*-Bu)-OC₇H₁₅ were dissolved in DMF (10 mL) in a 25 mL rb flask. The mixture was cooled to 0 °C and 2,4,6-trimethylpyridine (140 μL) and HBTU (143 mg) were added. The mixture was stirred at rt for 16 h. The mixture was diluted with CH₂Cl₂ (150 mL) and washed with 150 mL each of the following: H₂O, 1M NaHSO₄, H₂O × 3, 5% NaHCO₃, and H₂O. The CH₂Cl₂ solution was filtered through a 1:1 celite/MgSO₄ mixture. The solution was evaporated and chromatographed over a column of SiO₂ (eluent: 0%-10% MeOH in CHCl₃). Evaporation of the solvent followed by high vacuum for 16 h afforded **17** as a white solid (333 mg, 79% yield). MP: 125-128 °C. ¹H NMR: 0.88 (t, 9H); 1.16 (d, 18H); 1.26 (bs, 44H); 1.60 (bs, 6H); 2.11 (s, 4H); 3.11 (bs, 2H); 3.28 (bs, 2H); 3.57 (bs, 4H); 3.69 (m, 3H); 4.07 (m, 11H); 4.30 (s, 2H); 4.44 (m, 2H); 4.63 (m, 1H); 7.42 (bs, 2H); 7.71 (bs, 2H); 7.98 (bs, 1H); 8.26 (bs, 1H) ppm.

2.19 Preparation of (C₁₈H₃₇)₂NCOCH₂OCH₂CO(Gly)₃ProSer(*t*-Bu)GlySer(*t*-Bu)-OC₇H₁₅, **18**.

231 (C₁₈H₃₇)₂NCOCH₂OCH₂CO(Gly)₃OH (281 mg, 0.347 mmol) and 193 mg H-ProSer(*t*-Bu)GlySer(*t*-Bu)-OC₇H₁₅ were dissolved in DMF (10 mL) in a 25 mL rb flask. The mixture was cooled to 0 °C and 2,4,6-trimethylpyridine (140 μL) and HBTU (138 mg) were added. The mixture was stirred at rt for 16 h. The mixture was diluted with CH₂Cl₂ (150 mL) and washed with 150 mL each of the following: H₂O, 1M NaHSO₄, H₂O × 3, 5% NaHCO₃, and H₂O. The CH₂Cl₂ solution was filtered through a 1:1 celite/MgSO₄ mixture. The solution was evaporated and chromatographed over a column of SiO₂ (eluent: 0%-10% MeOH in CHCl₃). Evaporation of the solvent followed by high vacuum for 16 h afforded **18** as a white solid (399 mg, 85% yield). MP: 127-129 °C. ¹H NMR: 0.88 (t, 9H); 1.17 (d, 18H); 1.26 (bs, 65H); 1.60 (bs, 6H); 2.08 (bs, 4H); 3.09 (m, 2H); 3.27 (bs, 2H); 3.56-4.62 (m, 25H); 7.41 (m, 1H); 7.63 (bs, 1H); 7.74 (bs, 1H); 7.84 (bs, 1H); 8.09 (bs, 1H); 8.47 (bs, 1H) ppm.

2.20 Preparation of (C₁₂H₂₃)₂NCOCH₂CH₂CO(Gly)₃ProGlySer(*t*-Bu)Gly-OC₇H₁₅, **19**.

242 (C₁₂H₂₃)₂NCOCH₂CH₂CO(Gly)₃OH (531 mg, 0.850 mmol) was dissolved in DMF (10 mL) in a 25 mL rb flask. The mixture was cooled to 0 °C and 2,4,6-trimethylpyridine (337 μL) and HBTU (338 mg) were added. The mixture was stirred for 30 min and H-ProGlySer(*t*-Bu)Gly-OC₇H₁₅ (400 mg) was added. The mixture was stirred at rt for 16 h. The mixture was diluted with CH₂Cl₂ (250 mL) and washed with 250 mL each of the following: H₂O, 1M NaHSO₄, H₂O × 3, 5% NaHCO₃, and H₂O. The CH₂Cl₂ solution was filtered through a 1:1 celite/MgSO₄ mixture. The solution was evaporated and chromatographed over a column of SiO₂ (eluent: 5%-30% MeOH in CHCl₃). Evaporation of the solvent followed by high vacuum for 16 h afforded **19** as a white solid (811 mg, 88% yield). MP: 158-160 °C. ¹H NMR: 0.81 (t, 9H); 1.17 (bs, 54H); 1.53 (m, 8H); 1.85 (m, 8H); 2.10 (m, 7H); 2.45 (m, 4H); 3.13 (bs, 4H); 3.38-4.05 (m, 17H); 4.39 (m, 2H); 7.07 (d, 1H); 7.31 (bs, 2H); 7.44 (m, 2H); 7.88 (m, 2H) ppm.

2.21 Preparation of (C₁₈H₃₇)₂NCOCH₂CH₂CO(Gly)₃ProGlySer(*t*-Bu)Gly-OC₇H₁₅, **20**.

253 (C₁₈H₃₇)₂NCOCH₂CH₂CO(Gly)₃OH (674 mg, 0.850 mmol) was dissolved in DMF (10 mL) in a 25 mL rb flask. The mixture was cooled to 0 °C and 2,4,6-trimethylpyridine (337 μL) and HBTU (338 mg) were added. The mixture was stirred for 30 min and H-ProGlySer(*t*-Bu)Gly-OC₇H₁₅ (400 mg) was added. The mixture was stirred at rt for 16 h. The mixture was diluted with CH₂Cl₂ (250 mL) and washed with 250 mL each of the following: H₂O, 1M NaHSO₄, H₂O × 3, 5% NaHCO₃, and H₂O. The CH₂Cl₂ solution was filtered through a 1:1 celite/MgSO₄ mixture. The solution was evaporated and chromatographed over a column of SiO₂ (eluent: 5%-30% MeOH in CHCl₃). Evaporation of the solvent followed by high vacuum for 16 h afforded **20** as a white solid (892 mg, 84% yield). MP: 155-158 °C. ¹H NMR: 0.88 (t, 11H); 1.16 (s, 13H); 1.26 (bs, 74H); 1.60 (d, 6H); 2.12 (s, 4H); 2.63 (d, 4H); 3.22 (bs, 4H); 3.49-4.15 (m, 18H); 4.50 (bs, 2H); 7.33 (bs, 1H); 7.70 (bs, 3H); 8.12 (bs, 2H) ppm.

262
263
264
265
266
267
268
269
270
271
272

2.22 Preparation of $(C_{18}H_{37})_2NCOCH_2OCH_2CO(Gly)_3ProGlySer(t-Bu)Gly-OC_7H_{15}$, **21**.

$(C_{18}H_{37})_2NCOCH_2OCH_2CO(Gly)_3OH$ (515 mg, 0.636 mmol) was dissolved in DMF (10 mL) in a 25 mL rb flask. The mixture was cooled to 0 °C and 2,4,6-trimethylpyridine (337 μ L) and HBTU (338 mg) were added. The mixture was stirred for 30 min and H-ProGlySer(t-Bu)Gly-OC₇H₁₅ (400 mg) was added. The mixture was stirred at rt for 16 h. The mixture was diluted with CH₂Cl₂ (250 mL) and washed with 250 mL each of the following: H₂O, 1M NaHSO₄, H₂O \times 3, 5% NaHCO₃, and H₂O. The CH₂Cl₂ solution was filtered through a 1:1 celite/MgSO₄ mixture. The solution was evaporated and chromatographed over a column of SiO₂ (eluent: 5%-30% MeOH in CHCl₃). Evaporation of the solvent followed by high vacuum for 16 h afforded **21** as a white solid (712 mg, 88% yield). MP: 87-90°C. ¹H NMR: 0.88 (t, 11H); 1.17 (s, 10H); 1.26 (bs, 74H); 1.60 (d, 7H); 3.09-4.47 (m, 29H); 7.15 (bs, 1H); 7.67 (bs, 2H); 8.02 (bs, 3H) ppm.

273
274
275
276
277
278
279
280
281
282
283
284
285

2.23 Preparation of phospholipid vesicles and chloride release experiments.

1,2-Dioleoyl-*sn*-glycero-3-phosphocholine (DOPC) and 1,2-dioleoyl-*sn*-glycero-3-phosphate (DOPA) were obtained from Avanti Polar Lipids® as 25 mg in 2.5 mL CHCl₃ solutions. For each vesicle preparation, a dry film sample of DOPC:DOPA (15 mg, 7:3 w/w) was dissolved in 375 μ L Et₂O and then 375 μ L internal buffer (600 mM KCl, 10 mM N-2-hydroxyethylpiperazine-*N'*-2-ethanesulfonic acid (HEPES), pH adjusted to 7.00) was added. The mixture was sonicated for 30 s yielding an opalescent suspension. The diethyl ether was removed under low vacuum conditions at 30 °C for 2 hours. The resulting mixed micellar aqueous suspension was filtered through a 200 nm pore-size membrane filter 9 times using a small extruder to obtain a uniform size of vesicles. The filtered suspension was passed through a Sephadex G25 size exclusion column that had been equilibrated with external buffer (400 mM K₂SO₄, 10 mM HEPES, adjusted to pH 7.00) in order to eliminate the extra-vesicular chloride ions. The vesicles were collected and subsequently characterized by using dynamic light scattering. The size of the resulting purified vesicles was confirmed to be ~200 nm. The final lipid concentration was obtained by using a colorimetric determination of the phospholipid-ammonium ferrothiocyanate complex.

286
287
288
289
290
291
292
293

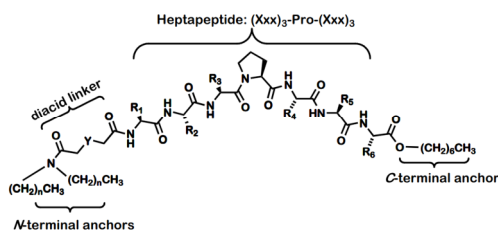
The chloride release from liposomes was assayed by using a chloride sensitive electrode (Accumet Chloride Combination Electrode). The electrode was immersed in the vesicle solution (0.31 mM) and allowed to equilibrate. After 5 minutes an aliquot of the compound solution was added to the vesicle suspension to a concentration of 65 μ M. The solution of compounds were prepared usually in a concentration of 9 mM to minimize the amount of 2-propanol and hence its effect on the liposomes. At the end of each experiment the 100 mL of a 2% Triton X-100 solution was added to the vesicle suspension to induce vesicular lysis and to obtain the total chloride concentration. The data collected (DigiData 1322A series interface and Axoscope 9.0 software) were then normalized to this value.

294
295
296
297
298
299
300
301
302
303

3. RESULTS AND DISCUSSION

3.1 The heptapeptide SATs.

As noted in the introduction, the essential elements of the SAT amphiphiles comprise four modules. These are illustrated in Figure 1. The twin hydrocarbon tails were designed to function as membrane anchors that mimic the fatty acid chains of phospholipids.[22] The diacid, shown in the figure as $\sim COCH_2YCH_2CO\sim$ is a linker intended to join the anchor groups with the heptapeptide and to mimic the glyceryl regime of phospholipids. The heptapeptide sequence was initially modeled on the putative selectivity filter of the ClC chloride-transporting protein. The C-terminal end of the heptapeptide is esterified with a *n*-heptyl group that prevents carboxyl ionization[23] and serves as a “secondary” membrane anchor.



304
305
306
307
308
309
310
311

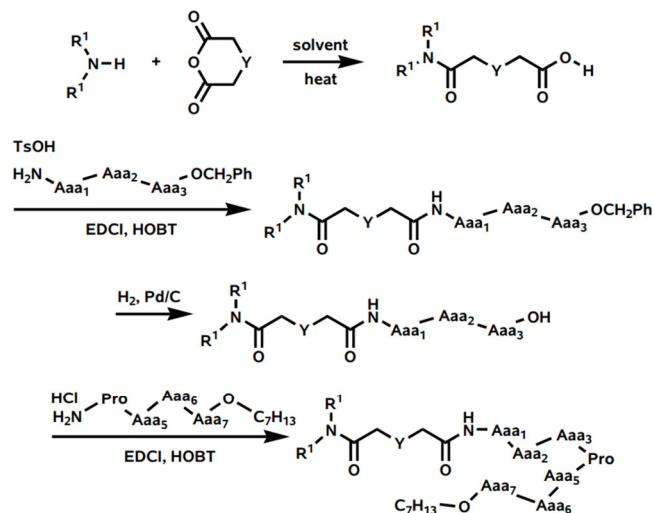
Figure 1. General structure for synthetic anion transporter (SAT) amphiphiles

3.2 Compounds used.

All of the compounds used in the present study are heptapeptides. In previous work, we surveyed the effects of varying the N-terminal twin anchor chain, the linker, and the C-terminal “secondary” anchor.[19] Likewise, we have examined the effect of changes in the peptide sequence while keeping the other variables constant. For the present study, the C-terminal anchor chain was always *n*-heptyl and the peptide always contained seven amino acids in the form

312 (Aaa)₃Pro(Aaa)₃. Early work showed that when proline at position 4 was replaced either by leucine or other cyclic amino
 313 acids, Cl⁻ ion release from liposomes was significantly reduced.[24]

314
 315 The compounds studied were typically prepared by reaction of a diamine (the *N*-terminal anchor) with a diacid anhydride
 316 to form the anchor and linker modules, R₂NCOCH₂YCH₂COOH in one step. In much of the early work and in the present
 317 report, diglycolic acid (Y = O) was the linker of choice. Alternately, thiadiglycolic acid (HOOCCH₂SCH₂COOH) anhydride
 318 or succinic anhydride (Y is absent) comprised the diacid linker element. A study of linker elements suggested that these
 319 three units were among the best to foster Cl⁻ ion release from liposomes.[25] The diamines were di-*n*-hexylamine, di-*n*-
 320 dodecylamine, or di-*n*-octadecylamine. Previous studies showed that shorter anchor chains afforded greater Cl⁻ ion
 321 release from liposomes, but at a cost of anion vs. cation selectivity.[26]



322
 323 **Scheme 1.** Synthesis of SATs (1-21). The abbreviations A_n and Aaa_n represent amino acids. Y may represent O,
 324 S, or be absent.

325
 326 The assembly of the SATs reported herein was accomplished in a straightforward and modular manner. As noted above,
 327 the incipient linker was a diacid converted into its anhydride. This was treated with a diamine to form the
 328 R₂NCOCH₂YCH₂COOH module. Commercially available triglycine or trialanine was coupled to proline using a standard
 329 HBTU protocol. Triglycine or other tripeptide was esterified with *n*-heptanol and the two fragments coupled to give
 330 R₂NCOCH₂YCH₂CON(Aaa)₇OC₇H₁₅. Where peptide protection was required, standard methods were employed.[27] The
 331 synthesis is illustrated in Scheme 1. The product SATs are shown in Table 1 with reference to Scheme 1.

332
 333

No.	Twin <i>N</i> -anchors	Linker ^b	Peptide	% Cl ⁻ release ^c
1	<i>n</i> -C ₆ H ₁₃	~COCH ₂ CH ₂ CO~	GGGP ₂ GGG	60
2	<i>n</i> -C ₁₀ H ₂₁	~COCH ₂ CH ₂ CO~	GGGP ₂ GGG	ND ^d
3	<i>n</i> -C ₁₂ H ₂₅	~COCH ₂ CH ₂ CO~	GGGP ₂ GGG	ND
4	<i>n</i> -C ₁₈ H ₃₇	~COCH ₂ CH ₂ CO~	GGGP ₂ GGG	70
5	<i>n</i> -C ₆ H ₁₃	~COCH ₂ OCH ₂ CO~	GGGP ₂ GGG	ND
6	<i>n</i> -C ₁₈ H ₃₇	~COCH ₂ OCH ₂ CO~	GGGP ₂ GGG	60
7	<i>n</i> -C ₁₂ H ₂₅	~COCH ₂ CH ₂ CO~	AAAP ₂ GGG	11
8	<i>n</i> -C ₁₈ H ₃₇	~COCH ₂ CH ₂ CO~	AAAP ₂ GGG	11
9	<i>n</i> -C ₁₂ H ₂₅	~COCH ₂ OCH ₂ CO~	AAAP ₂ GGG	28
10	<i>n</i> -C ₁₈ H ₃₇	~COCH ₂ OCH ₂ CO~	AAAP ₂ GGG	20
11	<i>n</i> -C ₁₈ H ₃₇	~COCH ₂ SCH ₂ CO~	AAAP ₂ GGG	20
12	<i>n</i> -C ₁₂ H ₂₅	~COCH ₂ CH ₂ CO~	GGGPSGS	13

13	<i>n</i> -C ₁₈ H ₃₇	~COCH ₂ CH ₂ CO~	GGGPSGS	10
14	<i>n</i> -C ₁₈ H ₃₇	~COCH ₂ O CH ₂ CO~	GGGPSGS	13
15	<i>n</i> -C ₁₂ H ₂₅	~COCH ₂ CH ₂ CO~	GGGPS(<i>t</i> -Bu)GS(<i>t</i> -Bu)	28
16	<i>n</i> -C ₁₈ H ₃₇	~COCH ₂ CH ₂ CO~	GGGPS(<i>t</i> -Bu)GS(<i>t</i> -Bu)	24
17	<i>n</i> -C ₁₂ H ₂₅	~COCH ₂ O CH ₂ CO~	GGGPS(<i>t</i> -Bu)GS(<i>t</i> -Bu)	30
18	<i>n</i> -C ₁₈ H ₃₇	~COCH ₂ O CH ₂ CO~	GGGPS(<i>t</i> -Bu)GS(<i>t</i> -Bu)	27
19	<i>n</i> -C ₁₂ H ₂₅	~COCH ₂ CH ₂ CO~	GGPGS(<i>t</i> -Bu)G	ND
20	<i>n</i> -C ₁₈ H ₃₇	~COCH ₂ CH ₂ CO~	GGPGS(<i>t</i> -Bu)G	ND
21	<i>n</i> -C ₁₈ H ₃₇	~COCH ₂ O CH ₂ CO~	GGPGS(<i>t</i> -Bu)G	ND

a. All compounds have a C-terminal *n*-heptyl anchor (see Figure 1). **b.** Linker heteroatoms are in bold type for clarity. **c.** Chloride release from DOPC:DOPA (7:3) liposomes mediated by SATs (see Experimental section for details). **d.** ND means not determined under these conditions.

334

335

3.3 Anion transport.

336

337

338

339

340

341

342

343

344

345

346

347

348

349

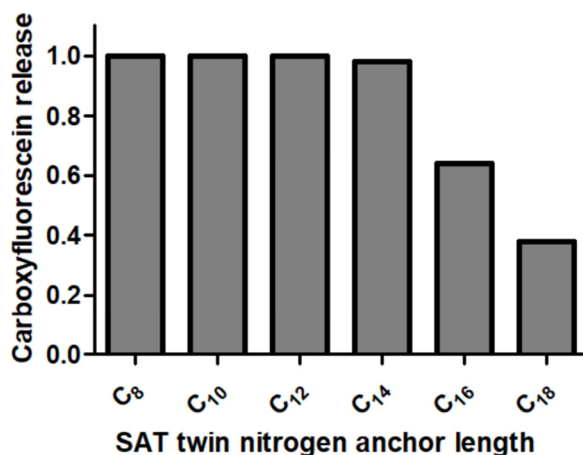
350

351

352

Anion release from liposomes was studied in various ways. The anion most commonly assessed was Cl⁻, which was detected as egress from DOPC:DOPA (7:3) liposomes (0.31 mM) mediated by SATs (65 μM at pH 7), using a Cl⁻-selective electrode. Alternately, the chloride selective dye lucigenin was used to detect Cl⁻ transport.[15] Fluorescein transport was studied as well. Fluorescein is often used as a surrogate for Cl⁻ because it can readily be detected at low concentrations.

An example of how the anchor chain (R) length in R₂NCOCH₂YCH₂CO-G₃PG₃-OCH₂Ph affects carboxyfluorescein (CF) release is shown in Figure 2. This is a convenient experiment because CF within vesicles is self-quenched. The highly fluorescent dye that emerges is readily detectable by fluorimetry. The di-*n*-alkyl chains that comprise the *N*-terminal anchors for the SAT ranged in length in this experiment from *n*-octyl to *n*-octadecyl. The experiment was arbitrarily terminated at 300 s, by which time the shortest chain compounds had released all of the dye. The 100% release value was determined by using Triton X-100 detergent to lyse the vesicles. The total dye was set to a value of 100% and compared to the amount released prior to lysis. Release is then expressed as a percentage. Figure 2 shows the length dependence of the “R” *N*-terminal anchor chains in R₂NCOCH₂OCH₂COG₃PG₃OCH₂Ph. Although the graph shows CF release, generally similar behavior has been observed for Cl⁻ release from liposomes when using Cl⁻-selective electrodes or lucigenin.[15]



353

354

355

356

357

358

359

Figure 2. Carboxyfluorescein release from DOPC:DOPA (7:3) liposomes (0.31 mM) mediated by R₂NCOCH₂OCH₂COG₃PG₃OCH₂Ph (65 μM at pH 7) in which the twin *N*-terminal anchor chains (R₂) range from *n*-octyl to *n*-octadecyl. The values reflect release at 300 s.

It should be noted that the compounds recorded in Table 1 and the compounds used in the CF release-rate study shown in Figure 2 differ from **1-21** in the C-terminal anchor. A study of the effect of variations in the C- and *N*-terminal chains (R¹) and C-terminal (R²) anchors in R₁²NCOCH₂OCH₂COG₃PG₃OR² has previously been reported.[28]

360 The C-terminal anchors (R²) included O-Et, O-*n*-heptyl, O-benzyl, O-methylenecyclohexyl, and O-*n*-octadecyl. The two
361 most favorable for ion transport were O-*n*-heptyl and O-benzyl. Similar, although not identical, behavior was observed for
362 these two seven-carbon C-termini. Thus, the comparison of Cl⁻ release data shown in Table 1 and the CF release data
363 plotted in Figure 2 are relevant to each other and to the results presented here.
364

365 3.4 Experimental plant studies.

366 *Arabidopsis thaliana* is the best known and most widely studied experimental plant. The most commonly used strain,
367 "Col-0," for which the entire genome is known, was used in the present study.[29] The growth medium was sterilized agar
368 containing plant nutrient plus sucrose or "PNS" as described in the experimental section. Approximately 20 seeds were
369 germinated on each plate and each experiment was conducted in at least triplicate. This resulted in each data point
370 representing 60 or more observations. Plants were allowed to grow under continuous white light for 11 days, at which
371 time the root properties were determined by visual analysis using a dissecting microscope.
372

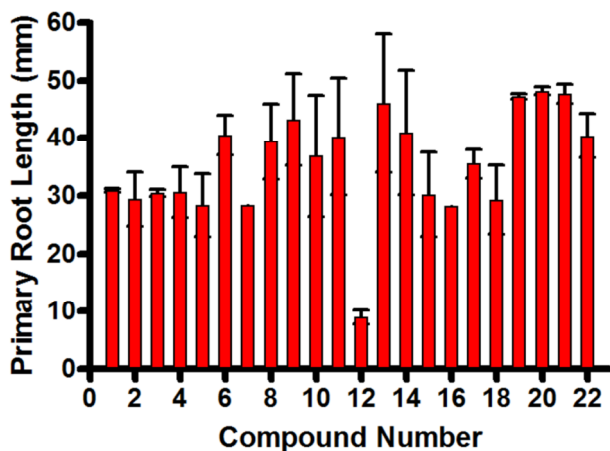
373 The data reported are the primary root length, measured in millimeters, and the number of lateral roots, assessed visually.
374 The *lateral root density* is an arbitrarily defined, unit-less value obtained by dividing the number of lateral roots by the
375 length of the primary root in millimeters. Thus, if the average length for 60 plants of the primary root is 35 mm and the
376 average number of lateral roots counted is 5.25, then the lateral root density would be (5.25/35 =) 0.15. Similarly, if the
377 average primary root length is 45 mm and the average number of lateral roots is 6.75, the lateral root density would be
378 (6.75/45 =) 0.15. The numbers shown were deliberately chosen to illustrate the possibility of accidental coincidence.
379

380 3.4.1 Controls.

381 Approximately 60 plants were grown on PNS media (no additives). Root lengths and the number of lateral roots were
382 recorded for each plant. The data points were averaged to obtain the following baseline values: primary root length = 40.4
383 ± 3.8 mm and number of lateral roots = 6.1 ± 0.8, respectively. The experimentally determined lateral root density
384 determined as the control value based on these observations is (6.1/40.6 =) 0.15.
385

386 The test compounds were added to the growth medium using an amount of DMSO equal to 0.2% of the final solution
387 volume. A control (60 plants) for DMSO at this concentration showed no effect on germination, growth, or on root
388 morphology compared to the PNS control absent DMSO (data not shown). This step was critical as DMSO is known to
389 affect membrane permeability[30] and, as a consequence, biological activity if the concentration is sufficiently high.[31]
390 Each SAT was added to a concentration of 50 μM in the PNS/agar growth medium. This value was chosen so that the
391 effect of SATs, if any, on *A. thaliana* could be compared with results previously obtained with hydrophiles.[6]
392

393 2,4-Dichlorophenoxyacetic acid (2,4-D) is a well-known broad leaf herbicide. It mimics the action of the natural growth
394 hormone indoleacetic acid. 2,4-D acts by overstimulating growth with an ultimately toxic effect. It was used as a positive
395 control in the present study. Based on the extreme difference in structure between 2,4-D and SATs, any effect of the latter
396 seems likely to occur by a different mechanism. 2,4-D was present in the PNS medium at a concentration of 100 nM and
397 plants were grown as noted above. This synthetic hormone significantly decreased both primary root length and lateral
398 root number to 3.9 ± 0.6 mm and 3.4 ± 0.6, respectively. The calculated lateral root density in this case is (3.4/3.9=) 0.85
399 (control = 0.15).

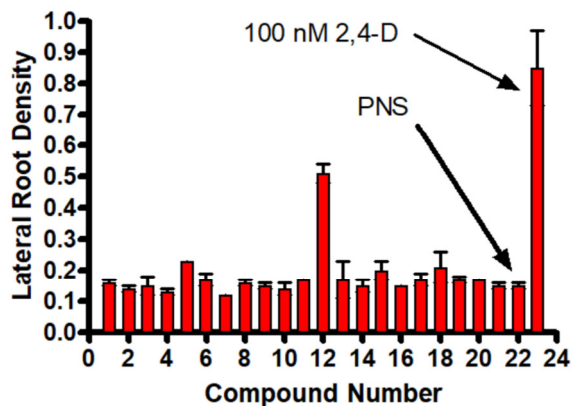


400 **Figure 3.** Plot of calculated lateral root density for compounds 1-21. The data for 22 (PNS) and 23 (2,4-D) are
401 controls (see text).
402

403 The results obtained for the 21 compounds included in this study are shown in the graph of Figure 3. The SATs are
404 identified by number (see Table 1). The designation 22 refers to the plant growth controls (average of ~60 plants). The

405 designation **23** refers to (~60) plants grown under the same conditions as controls with the toxin (2,4-D) added to the
406 growth media at the 100 nM level.
407

408 A similar plot is shown in Figure 4, in which the ordinate is primary root length. In this case, the effect of 2,4-D is not
409 included, but position 22 again corresponds to control. The correspondence in shortened primary root length and higher
410 lateral root density for compound **12** is apparent. Other points deserve note and are discussed below in terms of
411 heptapeptide sequence.
412



413 **Figure 4.** Plot of primary root length (in mm) for compounds **1-21**. The data for **22** are for the control plants (see
414 text).
415

416 **3.4.2 SATs having a (Gly)₃Pro(Gly)₃ heptapeptide sequence.**

417 The SAT compounds that we have studied most extensively in the past have a (Gly)₃Pro(Gly)₃ heptapeptide
418 sequence.[32] These compounds were designed to be chloride ion transporters and planar bilayer conductance data
419 confirmed this function.[33] Compounds **1-6** all have the G₃PG₃ peptide sequence and C-terminal *n*-heptyl esters, but
420 differ both in the N-terminal anchor and linker chains. The primary root length and the number of lateral roots for **6** is
421 within experimental error of the PNS control. The average primary root length for **1-5** is 30 mm, which compares with 40.4
422 mm for the PNS control. there is thus a mild growth retardation, which we infer is a modest toxic effect.
423

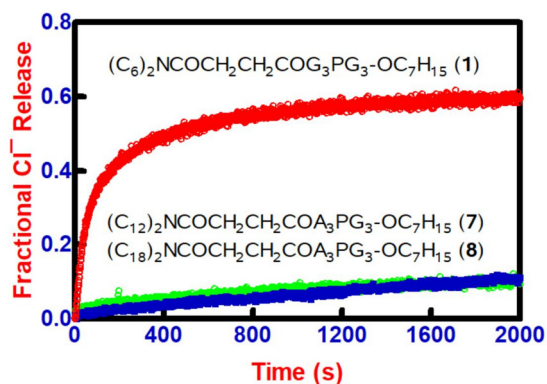
424 The shortest average root length for *A. thaliana* in the **1-5** series is exhibited by **5**, (C₆)₂NCOCH₂OCH₂COG₃PG₃OC₇. It is
425 28.4 ± 5.4 mm. This is significantly shorter than the control value of 40 mm. The average number of lateral roots observed
426 for **1-5** is 4.7. This compares to a control of 6.1 ± 0.8, a difference of nearly 30%. The calculated lateral root density for **1-5**
427 is (4.7/28.4 =) 0.165. This appears to differ little from the control value of 0.15, but this is a consequence of fewer lateral
428 roots being divided by a shorter primary root. Thus, the behavior of **1-5** is statistically, if not remarkably different from
429 control, or attributable to a specific cause. This is especially apparent for **5**, for which the lateral root density is (6.6/28.4 =)
430 0.23. Like **5**, **1** has *n*-hexyl side chains. Its structure is (C₆)₂NCOCH₂CH₂COG₃PG₃OC₇, and its lateral root density is 0.16.
431 Compound **6** in this family (C₁₈ anchors, diglycolic) fits within control parameters. We conclude that the biological effect is
432 greater for succinyl spacers and/or shorter anchor chains. This comports with the results of a study using planar bilayer
433 conductance showing that succinyl linkers generally foster greater conductance than do diglycoyl linkers.[34] We infer that
434 the Cl⁻ imbalance affects root morphology.
435

436 **3.4.3 SATs having the (Ala)₃Pro(Gly)₃ heptapeptide sequence.**

437 The heptapeptide sequence in compounds **7-11** is (Ala)₃Pro(Gly)₃. The peptide sequence in this group of compounds was
438 of interest because earlier studies showed that the strongest interactions with the peptide involved hydrogen bond
439 donation to Cl⁻ from to ⁵Gly and ⁷Gly.[35] No previous study explored variations in the peptide sequence on the N-
440 terminal side of proline. Compounds **7** and **8** have succinyl linkers and **9** and **10** are linked by diglycolic acid diamide. A
441 different linker is present in **11**, which has the structure (C₁₈)₂NCOCH₂SCH₂CO-A₃PG₃-OC₇. The linker here is
442 thiodiglycolic acid (Figure 1, Y = S). In short, no significant deviation from control was observed with **8-11** despite
443 variations in linker and anchor chain lengths. Compound **6** may be compared directly to **10**. Their structures (C₁₈ anchors,
444 diglycoyl linkers) are identical except for the G₃PG₃ (**6**) vs. A₃PG₃ (**10**) peptide sequences. Neither compound differs
445 significantly from the control in its biological effect on *A. thaliana*. As noted above, binding favored interactions on the C-
446 terminal side of proline. Thus, the G₃→A₃ alteration was not expected to show a significant difference in root development.
447

448 Compound **7**, however, which has the structure (C₁₂)₂NCOCH₂CH₂CO-A₃PG₃-OC₇, showed reduced primary root length
449 (28.4 mm) comparable to that observed for **1-5**, but an even smaller number of lateral roots (3.4). SATs **7** and **8** are

450 identical except for the *N*-terminal anchor chains, which are *n*-dodecyl in **7** and *n*-octadecyl in **8**. In an earlier study, we
 451 found that Cl⁻ transport was greater for (C_n)₂NCOCH₂CH₂CO-GGGPGGG-OCH₂Ph when C_n was *n*-dodecyl compared
 452 to *n*-octadecyl. It was concluded that the octadecyl compound was more selective, but less efficient, and that the dodecyl
 453 compound likely was transporting both Na⁺ and Cl⁻ ions.[36] If a similar effect on ion transport occurs in the case of **7**, it
 454 would explain the difference between the activities of **7** and **8**. Of course, this cannot be the only effect as the anchor
 455 chain difference is present in **9** and **10**, which are otherwise comparable, and their root profiles are similar to each other
 456 and to controls.
 457



458 **Figure 5.** Fractional release of Cl⁻ from DOPC:DOPA (7:3) liposomes (0.31 mM) mediated by succinic
 459 acid linked SATs **1**, **7**, and **8**.
 460

461 We also note that **10** and **11** (C₁₈ anchors, A₃PG₃ peptide) behave in a fashion similar to each other and to controls
 462 despite the difference in diglycolic (**10**) and thiadiglycolic (**11**) linkers. Taken together, some statistically significant
 463 differences in plant response to all glycine or alanine-glycine heptapeptides are observed, but these effects were minor.
 464

465 **3.4.4 SATs containing one or more serine residues in the heptapeptide sequence.**

466 Table 2, which shows details for compounds **12-21**, reveals a number of effects manifested by the presence of serine in
 467 the heptapeptide chain. The serines occur on the *C*-terminal side of proline and the hydroxyl group(s) are either protected
 468 (*t*-butylated) or free.
 469

470 Ten of the compounds reported here incorporate one or more serines into the heptapeptide sequence. The lateral root
 471 densities and the primary root lengths for **1-21** are plotted in Figures 3 and 4, respectively (above). Table 2 shows the
 472 compounds in three groups and includes the numerical information upon which the graph of Figure 4 is based. The
 473 peptides were prepared by coupling a G₃P fragment to either an SGS or GSG segment in which the serine hydroxyl
 474 groups were protected as the *t*-butyl ethers. As a result, we obtained **12-14** with free hydroxyl groups and **15-21** in their
 475 protected forms.
 476
 477

Table 2. Root Morphology Data for 12-21

Compound Number (50 μM)	Primary root length (mm)	Number of lateral roots	Lateral root density
PNS (±0.2% DMSO)	40.4 ± 3.8	6.1 ± 0.8	0.15 ± 0.01
2,4-D (100 nM)	3.9 ± 0.6	3.4 ± 0.6	0.85 ± 0.12
GGGPSGS			
Compound 12	9.0 ± 1.2	4.5 ± 0.4	0.51 ± 0.03
Compound 13	46.0 ± 12.0	8.7 ± 4.9	0.17 ± 0.06
Compound 14	40.9 ± 10.8	6.2 ± 2.4	0.15 ± 0.02
GGGPS(tBu)GS(tBu)			
Compound 15	30.2 ± 7.3	5.8 ± 0.7	0.20 ± 0.03
Compound 16	28.3	5.9	0.15
Compound 17	35.5 ± 2.5	5.9 ± 0.2	0.17 ± 0.02
Compound 18	29.3 ± 5.9	5.2 ± 0.3	0.21 ± 0.05
GGPGS(tBu)G			
Compound 19	47.3 ± 0.5	7.9 ± 0.5	0.17 ± 0.01
Compound 20	48.2 ± 0.7	8.2	0.17
Compound 21	47.7 ± 1.7	6.8	0.15 ± 0.01

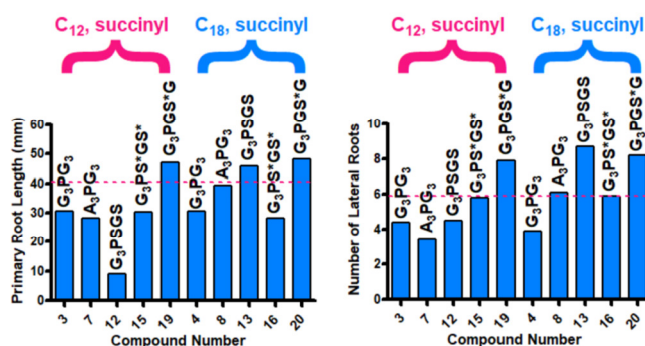
478

479 The simplest compounds in this group of three are **19-21**, in which the single serine in the G₃PGSG sequence is protected
 480 by *t*-butyl. Compounds **20** and **21** differ in having succinyl and diglycoyl linkers, but are otherwise identical. Compound **19**
 481 has the succinyl linker chain of **20**, but has twin dodecyl anchor chains rather than the octadecyl chains present in both **20**
 482 and **21**. The average primary root length measured for **19-21** was 47.7 mm and the variation in this value was small. The
 483 length is significantly longer (~20%) than the control value of 40.4 mm. Likewise, the average number of lateral roots (7.6)
 484 is about 25% greater than control. Since the lateral root density is higher and the primary root length is longer, the
 485 calculated lateral root density is similar to the control value. Overall, it appears that this group of SATs stimulates the
 486 growth of *A. thaliana* without significantly altering its growth characteristics of the whole plant. The results observed for the
 487 *bis*(serinyl) di-*t*-butyl ethers in **15-18** approximately parallel those observed for **1-5** and seem to exhibit the opposite of the
 488 effect observed for **19-21**.

489

490 3.4.5 Comparisons of heptapeptide sequence effects.

491 Two sets of compounds have identical *N*- and *C*-terminal anchor chains and succinyl linkers. They are **3, 7, 12, 15**, and **19**
 492 vs. **4, 8, 13, 16**, and **20**. Direct comparisons can be made between the following pairs: **3,4**; **7,8**; **12,13**; **15,16**; and **19,20**.
 493 These pairs have C₁₂ and C₁₈ *N*-terminal anchor chains, respectively, but otherwise are identical. The pairs differ from one
 494 another in the heptapeptide sequences. Figure 6 shows the effect of peptide sequence on primary root length (left) and
 495 lateral root density (right). Plants grown under control conditions have a primary root length of 40.4 mm, as indicated in
 496 the graph by the dashed line.



497

498 **Figure 6.** Left panel: Comparison of primary root lengths in pairs of compounds having C₁₂ and C₁₈ *N*-terminal
 499 anchors and succinyl linkers. The pairs have the following heptapeptide sequences: **3,4** (GGGPGGG); **7,8**
 500 (AAAPGGG); **12,13** (GGGPSGS); **15,16**; [GGGPS(*t*-Bu)GS(*t*-Bu)]; and **19,20** [GGGPS(*t*-Bu)G]. The dashed line
 501 indicates the primary root length of the controls. Right panel: Comparison of the number of lateral roots observed
 502 in pairs of compounds having C₁₂ and C₁₈ *N*-terminal anchors and succinyl linkers. The dashed line indicates the
 503 lateral root number of the controls. The symbol "S" indicates a serine having a *t*-butylated hydroxyl group. Error
 504 bars have been omitted for clarity.

505

506 Three compounds show primary root lengths significantly greater than controls. They are **13** (C₁₈, GGGPSGS), **19** and **20**
 507 [C₁₂ and C₁₈ GGGPS(*t*-Bu)G]. All three contain serine and all three stimulate primary root length to about the same
 508 extent (see Table 2). The C₁₈ SAT incorporating the AAAPGGG peptide (**8**) shows no effect on primary root length.
 509 Compounds **3, 4, 7, 15**, and **16** all affect *A. thaliana* growth by diminishing primary root length. That the **3,4** and **15,16**
 510 pairs behave the same suggests that it is the peptide sequence that is important rather than the *N*-terminal chain length.
 511 However, compound **7** reduces primary root length while its partner, **8**, shows no effect, suggesting that the peptide
 512 sequence alone cannot account for the difference. It is noted that this difference is relatively small when the error bars
 513 (not shown on graph) are taken into account.

514

515 The most striking results are observed with the **12,13** pair. In both cases, the heptapeptide sequence is GGGPSGS. The
 516 *N*-terminal anchor chains are C₁₂ in **12** and C₁₈ in **13**. The former shows a dramatic reduction in primary root length and
 517 the latter an increase outside of experimental error relative to control. In a previous study, it was found that the amide
 518 hydrogens of amino acids ⁵G and ⁷G were the key Cl⁻-binding donors when studied by NMR in a micellar matrix.[35] At
 519 present, we have no direct evidence that Cl⁻ – or any ion – binding is critical to the effect these compounds have on
 520 plants. Notwithstanding, the difference in effect on *A. thaliana* by **12** and **13** is dramatic and striking.

521

522 The results shown in Figure 6 parallel those of Figure 2. They show the effect of the same compounds on the number of
 523 lateral roots observed when administered to *A. thaliana*. As with primary root length, compounds **13, 19**, and **20** show
 524 enhancements relative to controls. As with primary root length, **8** shows no effect on lateral root number. In contrast,
 525 compounds **3, 4, 15**, and **16** showed similar, reduced primary root length, but the number of lateral roots is unaltered by

526 the presence of **15** and **16**. The lateral root number is diminished by the presence of **4** and **7** by an approximately equal
527 amount and **12** does not show such a dramatic effect as is apparent in primary root length.

528 **3.4.6 The activity of the GGGPSGS compounds, 12 and 13.**

529 The most striking observation made in this study is the effect of **12** and **13** on *A. thaliana*. Their structures are (C₁₂ or
530 C₁₈)₂NCOCH₂CH₂CO-G₃PSGS-OC₇. Four observations are remarkable about the SAT's biological activity. First, these
531 compounds dramatically reduce the primary root length of the test plants. Second, the number of lateral roots are
532 statistically below control, but not dramatically different from other, less active, heptapeptides. Third, the potent biological
533 activity of **12** is lost by protecting the two serine hydroxyl groups. Fourth, the longer *N*-terminal anchor chains essentially
534 void the effects observed in **12**. Indeed, longer-chained **13** shows a slightly longer primary root and significantly more
535 lateral roots than its shorter-chained congener.

536 The NMR study noted above showed that the glycines in the G₃PG₃ peptide's 5 and 7 positions were most intimately
537 involved with Cl⁻. The hydrogen atoms were not located in this NMR structure, but the conformation strongly
538 suggested >N—H hydrogen bond interactions. These may persist in **12** and be augmented by the two serine hydroxyls
539 that are in the 5 and 7 positions. This explanation would lead one to conclude that **12** and **13** would behave similarly.
540 Although their ability to release Cl⁻ from phospholipid liposomes is similar (**12**: 13%; **13**: 10%), both exhibit poor Cl⁻
541 transport. Compound **4**, in contrast, is identical to **13** except its heptapeptide is G₃PG₃ and its Cl⁻ release in 300 s is 70%.

542 Earlier studies showed that when otherwise identical SATs were compared, the compound with the C₁₂ anchors showed
543 greater transport efficacy and poorer selectivity than the analog with C₁₈ anchors. In addition, selectivity for Cl⁻ was lost
544 by the C₁₂ compound suggesting that Na⁺ and Cl⁻ were both being transported. The presence of cations and anions
545 within the channel could account for a difference in biological activity, but the loss of selectivity observed in that study was
546 accompanied by higher overall transport that is not observed here. It remains unclear why several of the serine-containing
547 SATs show both longer primary roots and an increased number of lateral roots.

548 **3.4.7 Comparison of SAT antibacterial activity with the action on A. thaliana.**

549 Compounds **1-21** were studied to determine if they exhibited toxicity to the K-12 strain of *Escherichia coli*. In these
550 experiments, the minimum inhibitory concentration was determined by using the Clinical and Laboratory Standards
551 Institute M07-A9 protocol.[37] None of the SATs reported here showed any toxicity to *E. coli* at concentrations below 256
552 μM (data not shown). Of course, *A. thaliana* and *E. coli* are classified in different biological domains so this difference in
553 activity may be expected. Notwithstanding, our previous observation that hydraphile pore-formers, which transport cations
554 rather than anions, are toxic to bacteria and show a significant effect on *A. thaliana* led us to anticipate a different
555 outcome.

556 **3.4.8 Comparison of SATs with Lariat Ethers and Hydraphiles.**

557 Previous work evaluated the ability of lariat ethers¹⁰ or hydraphiles⁶ to affect root morphology in *A. thaliana*. Hydraphiles
558 showed a general correlation between cation transport efficacy and increased lateral root development. Several of the
559 lariat ethers tested were known transporters, but were found to show clear evidence (planar bilayer conductance) for pore
560 formation. It was inferred in both cases that ion transport was affected leading to root alterations by a mechanism different
561 from that controlled by auxins. The SATs were designed to conduct Cl⁻ and considerable evidence confirms that. In terms
562 of activity in the development of *A. thaliana*, we conclude that the compounds that exhibit the greatest effect are those that
563 can also transport cations (short *N*-anchors) or interact effectively with endogenous cations (serine containing peptides).

564 **4. CONCLUSIONS**

565 The SATs are Cl⁻-selective pore-formers that generally have little effect on the root morphology of *A. thaliana*. The
566 exceptions are notable, however. These fall into three categories. First, the G₃PG₃ peptides all inhibit both primary root
567 growth and the number of lateral roots that form. The fact that root length is compromised without compensatory lateral
568 root development suggests a toxic effect. Second, the placement of two serines having pendant hydroxyl groups on the C-
569 terminal side of proline seems ideal to interact with cations as well as anions and exhibits the most dramatic effect on root
570 development. The third observation is that when the serine hydroxyl groups are protected, plant growth is stimulated. We
571 conclude that the SATs are generally biologically active in this context, but that the greatest effects are apparent when
572 interactions with cations, rather than anions, are possible.

573 **ACKNOWLEDGEMENTS**

574 We gratefully acknowledge support of this work by the National Science Foundation under grants CHE 1307324, CHE
575 1710549.

586
587
588
589
590
591
592
593
594
595
596
597
598
599
600
601
602
603
604
605
606
607
608
609
610
611
612
613
614
615
616
617
618
619
620
621
622
623
624
625
626
627
628
629
630
631
632
633
634
635
636
637
638
639
640
641

COMPETING INTERESTS

A patent application has been submitted, the rights to which are held by the Curators of the University of Missouri. Otherwise, no competing interests exist.

AUTHORS' CONTRIBUTIONS

All authors read and approved the final manuscript.

REFERENCES

- (a) Gokel, G. W.; Negin, S., Synthetic membrane active amphiphiles, *Adv. Drug. Deliv. Rev.* 2012;64(9):784-96. (b) Gokel, G. W.; Negin, S., Synthetic Ion Channels: From Pores to Biological Applications *Acc. Chem. Res.* 2013, 46 (12), 2824–2833.
- (a) Ugras, H. I.; Cakir, U.; Azizoglu, A.; Kilic, T.; Erk, C., Experimental, Theoretical and Biological Activity Study on the Acyl-Substituted Benzo-18-crown-6, Dibenzo-18-crown-6 and Dibenzo-24-crown-8 *J. Incl. Phenom. Macrocyclic Chem.* 2006, 55, 159-165. (b) Huang, S. T.; Kuo, H. S.; Hsiao, C. L.; Lin, Y. L., Efficient synthesis of 'redox-switched' naphthoquinone thiol-crown ethers and their biological activity evaluation *Bioorg. Med. Chem.* 2002, 10, 1947-52. (c) Sadeghian, A.; Seyedi, S. M.; Sadeghian, H.; Hazrathoseyni, A.; Sadeghian, M., Synthesis, biological evaluation and QSAR studies of some new thioether-ester crown ethers, *J. Sulfur Chem.* 2007, 28, 597-605. (d) Eshghi, H.; Rahimizadeh, M.; Zokaei, M.; Eshghi, S.; Eshghi, S.; Faghihi, Z.; Tabasi, E.; Kihanyan, M., Synthesis and antimicrobial activity of some new macrocyclic bis-sulfonamide and disulfides, *Eur. J. Chem.* 2011, 2, 47-50. (e) Zaim, O.; Aghatabay, N. M.; Gurbuz, M. U.; Baydar, C.; Dulger, B., Synthesis, structural aspects, antimicrobial activity and ion transport investigation of five new [1+1] condensed cycloheterophane peptides, *J. Incl. Phenom. Macrocycl. Chem.* 2014, 78, 151-159. (f) Le, T. A.; Truong, H. H.; Thi, T. P. N.; Thi, N. D.; To, H. T.; Thia, H. P.; Soldatenkov, A. T., Synthesis and biological activity of (gamma-arylpyridino)-dibenzoaza-14-crown-4 ethers, *Mendeleev Commun.* 2015, 25, 224-225. (g) Gumus, A.; Karadeniz, S.; Ugras, H. I.; Bulut, M.; Cakir, U.; Gorend, A. C., Synthesis, Complexation, and Biological Activity Studies of 4-Aminomethyl-7,8-dihydroxy Coumarines and Their Crown Ether Derivatives, *J. Heterocyclic Chem.* 2010, 47, 1127-1133. (h) Ozay, H.; Yildiz, M.; Unver, H.; Dulger, B., Synthesis, spectral studies, antimicrobial activity and crystal structures of phosphaza-lariat ethers, *Asian J. Chem.* 2011, 23, 2430-2436. (i) Kiraz, A.; Yildiz, M.; Dulger, B., Synthesis and characterization of crown ethers, *Asian J. Chem.* 2009, 21, 4495-4507. (j) Konup, L. A.; Konup, I. P.; V. E. Sklyar; Kosenko, K. N.; V. P. Gorodnyuk; Fedorova, G. V.; Nazarov, E. I.; Kotlyar, S. A., Antimicrobial activity of aliphatic and aromatic crown-ethers, *Khimiko-farmatsevticheskii Zhurnal* 1989, 23, 578-583. (k) Devinsky, F.; Lacko, I.; Inkova, M., Preparation of antimicrobially active amphiphilic azacrownethers of amine oxide and quaternary ammonium salt type, *Die Pharmazie* 1990, 45, 140. (l) Devinsky, F.; Devinsky, H., Czechoslovakia Patent 274 873 issued November 12, 1991. (m) Ugras, H. I.; Cakir, U.; Azizoglu, A.; Kilic, T.; Erk, C., Experimental, Theoretical and Biological Activity Study on the Acyl-Substituted Benzo-18-crown-6, Dibenzo-18-crown-6 and Dibenzo-24-crown-8, *J. Incl. Phenom. Macrocyclic Chem.* 2006, 55, 159-165. (n) Kato, N., Antibacterial action of alkyl-substituted crown ethers, *Kenkyu Kiyo - Konan Joshi Daigaku* 1985, 585-96. (o) Tso, W.-W.; Fung, W.-P.; Tso, M.-Y. W., Variability of crown ether toxicity, *J. Inorg. Biochem.* 1981, 14, 237-244.
- (a) Plotnikova, E. K.; Golovenko, N. Y.; Zin'kovskii, V. G.; Luk'yanenko, N. G.; Zhuk, O. V.; Basok, S. S., Transport and metabolism of a membrane-active complexon in mice, *Voprosy Meditsinskoi Khimii* 1987, 33, 62-66. (b) Timofeeva, S. E.; Voronina, T. A.; Karaseva, T. L.; Golovenko, N. Y.; Garibova, T. L.; Luk'yanenko, N. G., Psychotropic effects of some derivatives of N-crown ethers *Farmakologiya i Toksikologiya (Moscow)* 1986, 49, 13-15. (c) Van'kin, G. I.; Lukoyanov, N. V.; Galenko, T. G.; Raevskii, O. A., Pharmacologic activity of crown ethers, *Khimiko-Farmatsevticheskii Zhurnal* 1988, 22,

642 962-5. (d) Lukoyanov, N. V.; Van'kin, G. I.; Sapegin, A. M.; Raevskii, O. A.,
643 Physicochemical modeling of structure-activity relations. *Macrocyclic anticonvulsants*,
644 *Khimiko-farmatsevticheskii Zhurnal* 1990, 24, 48-51. (e) Adamovich, S. N.; Mirskova,
645 A. N.; Mirskov, R. G.; Perminova, O. M.; Chipanina, N. N.; Aksamentova, T. N.;
646 Voronkov, M. G., New Quaternary Ammonium Salts and Metal Complexes of
647 Organylheteroacetic Acids with Diaza-18-crown-6 Ether, *Russ. J. Gen. Chem.* 2010,
648 80, 1007-1010. (f) Kralj, M.; Majerski, K.; Ramljak, S.; Marjanovic, M., United States
649 Patent 8,389,505, Issued March 5, 2013. (g) Harris, E. J.; Zaba, B.; Truter, M. R.;
650 Parsons, D. G.; Wingfield, J. N., Specificities of cation permeabilities induced by some
651 crown ethers in mitochondria, *Arch. Biochem. Biophys.* 1977, 182, 311-320.

652 4 (a) Huang, D.; Wang, D.; Fu, T.; Que, R.; Zhang, J.; Huang, L.; Ou, H.; Zhang, Z.,
653 Effects of crown ethers on the K⁺ and Na⁺ transport of plant roots (1) Effect of benzo-
654 15-crown-5 on the K and Na transport of wheat roots, *J. Nanjing Univ. (Nat. Sci.)* 1980,
655 33-44. (b) Pemadasa, M. A., Effects of benzo-18-crown-6 on abaxial and adaxial
656 stomatal opening and its antagonism with abscisic acid, *New Phytol.* 1983, 93, 13-24.
657 (c) Macklon, A. E. S.; Sim, A.; Parsons, D. G.; Truter, M. R.; Wingfield, J. N., Effects of
658 some cyclic 'crown' polyethers on potassium uptake, efflux and transport in excised
659 root segments and whole seedlings *Ann. Bot.* 1983, 52, 345-356. (d) Huang, Z.; Yu, Z.;
660 Shu, J., The progress in the study on saturated urushiol crown ethers, *Organic*
661 *Chemistry* 1985, 6, 497-502. (e) Yuan, W.; Huang, Z.; Ruifeng, H., Effects of crown
662 ether on some physiological properties and economic characteristics of spikes of
663 wheat and panicles of rice, *Wuhan Univ. J. Nat. Sci.* 1996, 1, 259-262.

664 5 (a) Leong, B. K.; Ts'o, T. O.; Chenoweth, M. B., Testicular atrophy from inhalation of
665 ethylene oxide cyclic tetramer, *Toxicol. Appl. Pharmacol.* 1974, 27, 342-54. (b)
666 Takayama, K.; Hasegawa, S.; Sasagawa, S.; Nambu, N.; Nagai, T., Apparent oral
667 toxicity of 18-crown-6 in dogs, *Chem. Pharm. Bull.* 1977, 25, 3125-3130. (c)
668 Hendrixson, R. R.; Mack, M. P.; Palmer, R. A.; Ottolenghi, A.; Ghirardelli, R. G., Oral
669 toxicity of the cyclic polyethers--12-crown-4, 15-crown-5, and 18-crown-6--in mice,
670 *Toxicol. Appl. Pharmacol.* 1978, 44, 263-8. (d) O'Neil, M.J. (Ed.), *The Merck Index*,
671 14th Edition, Merck & Company, 2006, entry 851. (e) Takayama, K.; Hasegawa, S.;
672 Sasagawa, S.; Nambu, N.; Nagai, T., Dissolution profile and bioavailability of
673 sulfamonomethoxine/18-crown-6 complex in comparison with sulfamonomethoxine
674 anhydrate and hydrate *Chem. Pharm. Bull.* 1978, 26, 96-100. (f) Plotnikova, E. K.;
675 Golovenko, N. Y.; Zin'kovskii, V. G.; Luk'yanenko, N. G.; Zhuk, O. V.; Basok, S. S.,
676 Transport and metabolism of a membrane-active complexon in mice, *Voprosy*
677 *Meditsinskoi Khimii* 1987, 33, 62-66. (g) Timofeeva, S. E.; Voronina, T. A.; Karaseva,
678 T. L.; Golovenko, N. Y.; Garibova, T. L.; Luk'yanenko, N. G., Psychotropic effects of
679 some derivatives of N-crown ethers, *Farmakologiya i Toksikologiya (Moscow)* 1986,
680 49, 13-15. (h) Van'kin, G. I.; Lukoyanov, N. V.; Galenko, T. G.; Raevskii, O. A.,
681 Pharmacologic activity of crown ethers, *Khimiko-Farmatsevticheskii Zhurnal* 1988, 22,
682 962-5. (i) Lukoyanov, N. V.; Van'kin, G. I.; Sapegin, A. M.; Raevskii, O. A., Modeling
683 The Structure-Activity Relationship. V. Antihypoxic And Anticonvulsant Activity Of
684 Crown Ethers, *Khimikofarmat-sevticheskii Zhurnal* 1990, 24, 48-51.

685 6 Patel, MB; Stavri, A.; Curvey, N. S.; Gokel, G. W., Hydraphile synthetic ion channels
686 alter root architecture in *Arabidopsis thaliana*, *Chem. Commun.* 2014, 50, 11562-
687 11564.

688 7 Patel, MB, Negin, S, Stavri, A, Gokel, GW, Supramolecular Cation Transporters Alter
689 Root Morphology in the *Arabidopsis Thaliana* Plant, *Inorganica Chimica Acta*, 2017,
690 468, 183-191.

691 8 Gao, K.; Chen, F.; Yuan, L.; Zhang, F.; Mi, G., A comprehensive analysis of root
692 morphological changes and nitrogen allocation in maize in response to low nitrogen
693 stress. *Plant Cell Environ.* 2015, 38 (4), 740-750.

694 9 Fan, J.-W.; Du, Y.-L.; Turner, N. C.; Wang, B.-R.; Fang, Y.; Xi, Y.; Guo, X.-R.; Li, F.-
695 M., Changes in root morphology and physiology to limited phosphorus and moisture in

- 696 a locally-selected cultivar and an introduced cultivar of *Medicago sativa* L. growing in
697 alkaline soil. *Plant Soil* 2015, 392, 215-226.
- 698 10 Bernardy, K.; Farias, J. G.; Dorneles, A. O. S.; Pereira, A. S.; Schorr, M. R. W.;
699 Thewes, F. R.; Londero, J. E. L.; Nicoloso, F. T., Changes in root morphology and dry
700 matter production in *Pfaffia glomerata* (Spreng.) Pedersen accessions in response to
701 excessive zinc. *Rev. Bras. Pl. Med.*, Campinas 2016, 18 (2, Supl. 1), 613-620.
- 702 11 Marastoni, L.; Sandri, M.; Pii, Y.; Valentinuzzi, F.; Cesco, S.; Mimmo, T., Morphological
703 Root Responses and Molecular Regulation of Cation Transporters Are Differently
704 Affected by Copper Toxicity and Cropping System Depending on the Grapevine
705 Rootstock Genotype. *Front. Plant. Sci* 2019, 10, Article 946.
- 706 12 Belatus, E. L., Morphological Features, Cation Exchange Capacity, and Osmotic
707 Pressure for Different Banana Root Segments. *Middle East J. Agriculture* 2018, 7, 21-
708 26.
- 709 13 Strohm, A. K.; Vaughn, L. M.; Masson, P. M., Natural variation in the expression of
710 ORGANIC CATION TRANSPORTER 1 affects root length responses to cadaverine in
711 *Arabidopsis*. *J. Exp. Botany* 2015, 66 (3), 853-862.
- 712 14 Gokel, G.W.; Daschbach, M.M.; "Synthetic Amphiphilic Peptides that Self-assemble to
713 Membrane-active Anion Transporters," in Bianchi, A.; Bowman-James, K.; Garcia-
714 España, E. *Supramolecular Chemistry of Anions*; 2nd Edition, Wiley-VCH: New York,
715 2012, 45-62.
- 716 15 Riccardo Ferdani, R, Li, R, Pajewski, R, Pajewska, J, Winter, RK, Gokel, GW,
717 Transport of chloride and carboxyfluorescein through phospholipid vesicle membranes
718 by heptapeptide amphiphiles. *Org. Biomol. Chem.*, 2007, 5, 2423–2432.
- 719 16 Schlesinger, P. H.; Ferdani, R.; Liu, J.; Pajewska, J.; Pajewski, R.; Saito, M.; Shabany,
720 H.; Gokel, G. W., SCMTR: a chloride-selective, membrane-anchored peptide channel
721 that exhibits voltage gating. *J. Am. Chem. Soc.* 2002, 124 (9), 1848-9.
- 722 17 Djedovic, N.; Ferdani, R.; Harder, E.; Pajewska, J.; Pajewski, R.; Schlesinger, P. H.;
723 Gokel, G. W., The C-terminal ester of membrane anchored peptide ion channels
724 affects anion transport. *Chem. Commun.* 2003, (23), 2862-3.
- 725 18 Ferdani, R.; Pajewski, R.; Djedovic, N.; Pajewska, J.; Schlesinger, P. H.; Gokel, G. W.,
726 Anion Transport in Liposomes is Altered by Changes in the Anchor Chains and the
727 Fourth Amino Acid of Heptapeptide Ion Channels. *New J. Chem.* 2005, 29, 673-680.
- 728 19 Schlesinger, P. H.; Djedovic, N. K.; Ferdani, R.; Pajewska, J.; Pajewski, R.; Gokel, G.
729 W., Anchor chain length alters the apparent mechanism of chloride channel function in
730 SCMTR derivatives. *Chem. Commun.* 2003, (3), 308-309.
- 731 20 Pajewski, R.; Pajewska, J.; Li, R.; Daschbach, M. M.; Fowler, E. A.; Gokel, G. W., The
732 Effect of Midpolar Regime Mimics on Anion Transport Mediated by Amphiphilic
733 Heptapeptides. *New J. Chem.* 2007, 31, 1960-1972.
- 734 21 Pajewski, R.; Ferdani, R.; Pajewska, J.; Djedovic, N.; Schlesinger, P. H.; Gokel, G. W.,
735 Evidence for dimer formation by an amphiphilic heptapeptide that mediates chloride
736 and carboxyfluorescein release from liposomes. *Org. Biomol. Chem.* 2005, 3, 619-625.
- 737 22 Elliott, E.K.; Daschbach, M.M.; Gokel; G.W.; Aggregation behavior and dynamics of
738 synthetic amphiphiles that self-assemble to anion transporters, *Chem. Eur. J.* 2008,
739 14, 5871-5879.
- 740 23 You, L.; Ferdani, R.; Li, R.; Kramer, J.P.; Winter, R. E. K.; Gokel, G. W.; Carboxylate
741 anion diminishes chloride transport through a synthetic, self-assembled
742 transmembrane pore, *Chemistry – A European Journal*, 2008, 14(1), 382-396
- 743 24 Schlesinger, P. H.; Ferdani, R.; Pajewska, J.; Pajewski, R., Gokel, G. W.; Replacing
744 proline at the apex of heptapeptide-based chloride ion transporters alters their
745 properties and their ionophoretic efficacy, *New Journal of Chemistry*, 2003, 26, 60-
746 67.
- 747 25 Pajewski, R, Pajewska, J, Li, R, Fowler, EA, Gokel, GW, The Effect of Midpolar
748 Regime Mimics on Anion Transport Mediated by Amphiphilic Heptapeptides *New J.*
749 *Chem.*, 2007, 31, 1960–1972.

- 750 26 Pajewski, R; Ferdani, R; Schlesinger, PH.; Gokel, GW.; Chloride complexation by
751 heptapeptides: influence of C- and N-terminal sidechains and counterion Chem.
752 Commun., 2004, 160-161.
- 753 27 Grant, G. A. Synthetic Peptides: A User's Guide; Second edn.; Oxford University
754 Press: Oxford, 2002, 390 pp.
- 755 28 Ferdani, R.; Pajewski, R.; Djedovic, N.; Pajewska, J.; Schlesinger, P.H.; Anion
756 Transport in Liposomes Responds to Variations in the Anchor Chains and the Fourth
757 Amino Acid of Heptapeptide Ion Channels, Gokel, G.W.; New J. Chem., 2005, 29,
758 673–680.
- 759 29 *A. thaliana* Col 0 was obtained from The Arabidopsis Biological Resource Center
760 (ABRC) <https://abrc.osu.edu>.
- 761 30 (a) R. Notman, M. Noro, B. O'Malley, J. Anwar, Molecular basis for dimethylsulfoxide
762 (DMSO) action on lipid membranes, J. Am. Chem. Soc. 2006, 128, 13982–13983. (b)
763 R. Notman, W.K. den Otter, MG, Noro, WJ, Briels, JA, The permeability enhancing
764 mechanism of DMSO in ceramide bilayers simulated by molecular dynamics, Biophys.
765 J. 2007, 93, 2056–2068.
- 766 31 S. Negin, M.R. Gokel, M.B. Patel, S.L. Sedinkin, D.C. Osborn, G.W. Gokel, The
767 Aqueous Medium-Dimethylsulfoxide Conundrum in Biological Studies, RSC-Advances
768 2015, 5, 8088–8093.
- 769 32 (a) Djedovic, N.; Ferdani, R.; Harder, E.; Pajewska, J.; Pajewski, R.; Weber, M.E.;
770 Schlesinger, PH.; Gokel, GW.; The C- and N-Terminal Residues of Synthetic
771 Heptapeptide Ion Channels Influence Transport Efficacy Through Phospholipid
772 Bilayers, New J. Chem. 2005, 29, 291-305. (b) Ferdani, R.; Pajewski, R.; Djedovic, N.;
773 Pajewska, J.; Schlesinger, P.H.; and Gokel, G.W.; New J. Chem., 2005, 29, 673–680.
- 774 33 Schlesinger, P. H.; Ferdani, R.; Liu, J.; Pajewska, J.; Pajewski, R.; Saito, M.; Shabany,
775 H.; Gokel, GW, SCMTR: a chloride-selective, membrane-anchored peptide channel
776 that exhibits voltage gating, J. Am. Chem. Soc. 2002, 124, 1848-1849.
- 777 34 Minooie, F.; Martin, MD.; Fried, JR. Electrophysiological measurements reveal that a
778 succinyl linker enhances performance of the synthetic chloride channel SCMTR,
779 Chem. Commun. 2018, 54, 4689-4691.
- 780 35 Cook, GA, Pajewski, R, Aburi, M, Smith, PE, Prakash, O, Tomich, JM, Gokel, GW,
781 NMR structure and dynamic studies of an anion-binding, channel-forming
782 heptapeptide, J. Am. Chem. Soc. 2006, 128, 1633-1638.
- 783 36 Schlesinger, P. H.; Ferdani, R.; Pajewski, R.; Pajewska, J.; Gokel, G. W. A
784 hydrocarbon anchored peptide that forms a chloride-selective channel in liposomes,
785 Chem. Commun. 2002, 840-1.
- 786 37 Clinical and Laboratory Standards Institute: M07-A9, "Methods for dilution
787 antimicrobial susceptibility tests for bacteria that grow aerobically;" Approved standard,
788 ISBN 1-56238-784-7, www.clsi.org 2012, Ninth Edition.
- 789
790
791
792